Manuscrir	ot fo	r the	iournal	Fluid	Phase	Equilibria
manuscii	,, 10	1 0110	Journal	1 tutu	1 nusc	Lyaninoria

Pair correlation function of inhomogeneous hard sphere fluids

B. Götzelmann¹, S. Dietrich

 ${\it Fachbereich\ Physik,\ Bergische\ Universit\"{a}t\ Wuppertal},$

D-42097 Wuppertal, Germany

¹Corresponding author

Abstract

The two-point correlation function of inhomogeneous hard sphere fluids is analyzed within a certain version of weighted density functional theory. We have determined the direct correlation function and, based on the Ornstein-Zernicke equation, its inverse yielding the structure factor for such fluids confined by hard, structure-less, and parallel walls. We have also calculated the excess coverage and the finite size contribution to the free energy are computed as function of the slit width L for various bulk densities. In quantitative agreement with rigorous results the present version of density functional theory yields a constant and large but finite number density profile in the slit for the limiting case that L is reduced to the diameter of the hard spheres.

Keywords: statistical mechanics, solid-fluid equilibria, interfacial tension, correlation functions

1. Introduction

With the advent of new powerful neutron and synchroton sources diffuse scattering experiments of X-rays and neutrons from interfaces are realizable and give access to the total correlation function at these inhomogeneities [1]. In order to be able to interpret such data theoretical guidance is necessary. Here we provide a first step towards that goal by presenting the total correlation function of a hard sphere fluid close to hard walls. This simple model fluid captures the main features of the packing effects at short distances as they occur also in fluids governed by additional, attractive interactions. Furthermore the knowledge of the structural properties of hard sphere fluids is a prerequisite for treating attractive interactions pertubatively within a density functional theory approach. This system also has an importance of its own, because it can closely resemble the properties of colloidal suspensions, in which the correlation functions are directly accessible [2].

2. Theory

Density functional theory is based on the property of equilibrated systems, which are exposed to an external potential $V(\mathbf{R})$, that all measurable quantities are unique functionals of the number density profile $\rho(\mathbf{R})$ which minimmizes the grand canonical free energy functional

$$\Omega([\tilde{\rho}(\mathbf{R})]; \mu, T) = F_{ex}([\tilde{\rho}(\mathbf{R})]; T) + F_{id}([\tilde{\rho}(\mathbf{R})]; T) - \int d^3R \left(\mu - V(\mathbf{R})\right) \tilde{\rho}(\mathbf{R})$$
(1)

depending on the chemical potential μ and the temperatur $T=1/(k_B\beta)$.

 $F_{id}([\tilde{\rho}(\mathbf{R})];T) = \frac{1}{\beta} \int d^3R \,\tilde{\rho}(\mathbf{R})(\ln(\Lambda^3\tilde{\rho}(\mathbf{R})) - 1)$ is the free energy functional of an ideal gas with de Broglie wavelength Λ and $F_{ex}([\tilde{\rho}(\mathbf{R})],T)$ captures those contribu-

tions to the free energy of the system which are induced by the pair potential $\Phi(\mathbf{R})$ between the particles.

Derivatives of these functionals define the hierarchy of the direct correlation functions,

$$c^{(n)}([\rho(\mathbf{R})]; \mathbf{R}_1, \dots, \mathbf{R}_n) := -\beta \frac{\delta^n F_{ex}([\rho(\mathbf{R})], T)}{\delta \rho(\mathbf{R}_1) \dots \delta \rho(\mathbf{R}_n)},$$
(2)

and the one- and two-point correlation functions $(u(\mathbf{R}) = \mu - V(\mathbf{R}))$:

$$\rho(\mathbf{R}_1) := -\frac{\delta\Omega}{\delta u(\mathbf{R}_1)} = \langle \hat{\rho}(\mathbf{R}_1) \rangle, \quad G([\rho(\mathbf{R})]; \mathbf{R}_1, \mathbf{R}_2) := -\frac{1}{\beta} \frac{\delta^2\Omega}{\delta u(\mathbf{R}_1)\delta u(\mathbf{R}_2)}. \quad (3)$$

From Eq. (1) one obtains

$$c^{(1)}([\rho(\mathbf{R})]; \mathbf{R}_1) = \ln(\Lambda^3 \rho(\mathbf{R}_1)) - \beta u(\mathbf{R}_1)$$
(4)

$$c^{(2)}([\rho(\mathbf{R})]; \mathbf{R}_1, \mathbf{R}_2) = \frac{\delta(\mathbf{R}_1 - \mathbf{R}_2)}{\rho(\mathbf{R}_1)} - G^{-1}([\rho(\mathbf{R})]; \mathbf{R}_1, \mathbf{R}_2),$$
 (5)

where G^{-1} denotes the inverse of the two-point correlation function G. With the definition of the total correlation function,

$$h(\mathbf{R}_1, \mathbf{R}_2) = (G(\mathbf{R}_1, \mathbf{R}_2) - \delta(\mathbf{R}_1 - \mathbf{R}_2)\rho(\mathbf{R}_1))/(\rho(\mathbf{R}_1)\rho(\mathbf{R}_2)), \tag{6}$$

Eq. (5) leads to the Ornstein-Zernicke equation

$$h(\mathbf{R}_1, \mathbf{R}_2) = c(\mathbf{R}_1, \mathbf{R}_2) + \int d^3 R_3 c(\mathbf{R}_1, \mathbf{R}_3) \rho(\mathbf{R}_3) h(\mathbf{R}_3, \mathbf{R}_2).$$
 (7)

For a given functional $F_{ex}([\rho(\mathbf{R})];T)$ the total correlation function can be obtained by calculating the direct correlation function (Eq. (2)) and subsequently inverting the Ornstein-Zernicke equation (7).

In the following we consider hard spheres of diameter σ exposed to two structureless hard walls which are described by the external potential

$$V(\mathbf{R}) = \begin{cases} \infty & , \quad z < \sigma, \ z > L - \sigma \\ 0 & , \quad \sigma < z < L - \sigma \end{cases}$$
 (8)

Minimizing the functional $\Omega([\rho(\mathbf{R})]; \mu, T)$ (Eq. (1)) yields the density profile $\rho(\mathbf{R})$, which can be characterized by the excess coverage

$$\Gamma(L) := \int_{\sigma}^{L-\sigma} dz \left[\rho(z) - \rho_b \right]. \tag{9}$$

and the contact density $\rho(\sigma)$. The finite size contribution to the grand canonical potential $\Omega([\rho(\mathbf{R})]; \mu, T)$ is defined by

$$\gamma(L) := \lim_{A \to \infty} \frac{1}{A} \Omega([\rho(\mathbf{R})]; \mu, T) + (L - 2\sigma) P(\rho_b), \tag{10}$$

where $P(\rho_b)$ is the pressure and ρ_b is the number density of corresponding homogeneous bulk fluid at the same chemical potential. A is the cross section of the slit. These quantities obey the force relation

$$\rho(\sigma) = -\beta \left(\frac{\partial \gamma}{\partial L}\right)_{T,\mu} + \beta P(\rho_b) \tag{11}$$

and the adsorption relation

$$\Gamma(L) = -\left(\frac{\partial \gamma}{\partial \mu}\right)_{TL}.\tag{12}$$

These relations enable one to infer energies of the system from its structural properties. This facilitates the measurement of the surface tension γ [3], because the solvation force $\rho(\sigma)/\beta - P(\rho_b)$ is experimentally accessible, and it allows one to compute it from grand canonical simulations [4] which provide accurate data for $\Gamma(L)$. Within density functional theory these three routes will lead to the same result provided the exact functional is used. However, since only approximations thereof are available, in practice discrepancies between the different routes are to be expected. But, as shown in Ref [5], Eq. (11) still holds in the case of a weighted density approximation (WDA) of the excess free energy functional $F_{ex}([\rho(\mathbf{R})]; T)$.

Also Eq. (12) is still valid in this case, as one can see by taking the derivative of the grand canonical potential (Eq. (1))

$$\left(\frac{\partial\Omega}{\partial\mu}\right)_{T,L} = -\int d^3R \,\rho(\mathbf{R}) + \int_{\mathbb{R}^3} d^3R \,\left\{\frac{\delta F[\rho]}{\delta\rho(\mathbf{R}')} - (\mu - V(\mathbf{R}'))\right\} \,\frac{\partial\rho(\mathbf{R}')}{\partial\mu}.\tag{13}$$

According to Eq. (4) for an equilibrium profile the expression in curly brackets vanishes even in the case of an approximate version of F_{ex} . Differentiating Eq. (10) finally leads to

$$\left(\frac{\partial \gamma(L)}{\partial \mu}\right)_{T,L} = -\frac{1}{A} \int d^3 R \, \rho(\mathbf{R}) + (L - 2\sigma) \left(\frac{\partial P}{\partial \mu}\right)_T$$

$$= -\int_{\sigma}^{L-\sigma} dz \, (\rho(z) - \rho_b)$$

which is equivalent to the definition of the coverage (Eq. (9)).

3. Results

In the limit $L \to \infty$ the fluid at each wall reduces to a system consisting of a hard sphere fluid exposed to a single hard wall. This density profile was determined by minimizing Eq. (1) within the framework of the so-called LWDA approximation of the free energy functional [6] and is shown in Fig. 1(a). It is known to compare well with computer simulations [6]. Close to the wall the profile is rather different from the corresponding radial distribution function $g(\mathbf{R}_1, \mathbf{R}_2) := h(\mathbf{R}_1, \mathbf{R}_2) - 1$ in the bulk (compare Figs. 1 (a) and 1 (c)), but it has been proven [7] that at larger distances the decay and the period of the oscillations are the same.

The surface tension of a fluid exposed to a single wall, i. e. $\gamma(L \to \infty)/2$ as obtained from Eq. (10)), is given in Fig. 2. It compares very well with computer simulations [8, 9] and the scaled particle theory (SPT) [10]. The surface tension is negative and its absolute value increases with increasing bulk density.

For bulk densities well below the onset of prefreezing near the wall all correlation functions depend only on the transverse distance $r_{12} = \sqrt{(x_1 - x_2)^2 - (y_1 - y_2)^2}$ and the normal coordinates z_1 and z_2 , i. e. for example $g(\mathbf{R}_1, \mathbf{R}_2) = g(r_{12}, z_1, z_2)$. Figure 1 (d) displays the contour lines of the radial distribution function $g(r_{12}, z_1 = \sigma, z_2)$. It resembles the behavior of the bulk correlation function (Fig. 1 (c)), but for small distances $R = \sqrt{r_{12}^2 + (z_2 - \sigma)^2}$ significant deviations occur. The conditional singlet density $\rho(\mathbf{R}_1|\mathbf{R}_2) := \rho(z_2)g(r_{12}, z_1, z_2)$ provides additional insight. It corresponds to the density distribution of a hard sphere fluid close to a hard wall disturbed by the presence of a fixed hard sphere particle placed at \mathbf{R}_2 . A contour plot of $\rho(\mathbf{R}_1|\mathbf{R}_2)$ is shown in Fig 1 (b), thus combining Figs. 1 (a) and 1 (d). The dots and circles denote the maxima and minima, respectively. As contour lines corresponding to values larger than one are omitted, the dots whose position fullfill $z_2/\sigma < 3.5$ are situated in areas where the values of $\rho(\mathbf{R}_1|\mathbf{R}_2)$ are larger than one.

At a constant chemical potential μ , chosen to be the same as for a homogeneous hard sphere liquid whith $\rho_b\sigma^3=0.57$, the grand canonical potential was minimized for various slit widths $L/\sigma=2.025-8.0$. According to Fig. 3 the excess coverage and the finite size contribution to the free energy show oscillations characterized by a period of σ and an exponentially decaying envelope. Because of the force relation (Eq. 11) the same is true for the contact density $\rho(\sigma)$. In the limit $L \to 2$, it is known [11] that the density remains finite and is almost constant in the slit. An expansion of LWDA in terms of $\tilde{L} := L - 2\sigma$ reveals, that the above exact result is fullfilled in first order of \tilde{L} . (The same is true for other WDA's [12], but there are strong indications, that some of them [13] fail.) Within that expansion one obtains:

$$\rho(z=\sigma^+) = \Lambda^{-3} \exp(\frac{\mu}{kT})(1-\rho(\sigma)\pi\sigma^2\tilde{L} + O(\left(\frac{\tilde{L}}{\sigma}\right)^2)),$$

$$\Gamma(L \to 2\sigma)) = (L - 2\sigma) \left(\Lambda^{-3} \exp(\beta \mu) - \rho_b\right) + O\left(\left(\frac{L}{\sigma}\right)^2\right) \stackrel{L \to 2\sigma}{\to} 0,$$

and

$$-\gamma(L) = \left(\frac{1}{\beta}\rho(\sigma) - P_{PY}\right)(L - 2\sigma) + O\left(\left(\frac{\tilde{L}}{\sigma}\right)^2\right). \tag{14}$$

This implies that in the grand canonical ensemble in the limit $\tilde{L} \to 0$ the fluid is squeezed out of the slit and that the the number density < N > /A of the particles per area still contained inside the slit vanishes linearly as the width is decreased. Thus we conclude that the hard sphere fluid in a slit connected to a reservoir does not resemble the genuinely two-dimensional hard disc fluid. Only if the chemical potential diverges in a proper way or if one resorts to the canonical ensemble, a truley two-dimensional fluid can be formed.

The radial distribution function $g(r_{12}, z_1, z_2)$ of confined colloidal particles as a function of r_{12} parallel to the wall, i. e. $z_1 = z_2$, can be measured directly by means of video microscopy [2]. The analysis within the framework of LWDA reveals that in the case of a bulk density less than $0.68\sigma^3$ and for $L \gtrsim 5\sigma$ the correlation function $g(r_{12}, z_1 = \sigma, z_2 = z_1)$ is essentially equal to the one of the semi-infinite system. At a fixed slit width the correlation function depends sensitively on the normal coordinate $z_1 = z_2$. Thus a good depth resolution in such experiments is necessary. For a fixed width $L = 5.1\sigma$ and a corresponding bulk density $\rho_b = 0.545\sigma^3$ Fig. 4 displays the radial distribution function $g(r_{12}, z_1 = 1.64\sigma, z_2 = z_1)$. In the corresponding density profile the density $\rho(z_1 = 1.64\sigma)\sigma^3 = 0.409$ exhibits a local minima. There have been efforts [14, 15] to approximate the correlation function of a inhomogeneous liquid such that in the case $z_1 = z_2$ it reduces to $g(r_{12}, z_1, z_2) \approx g_b(r = r_{12}; \rho_b = \rho(z_1))$. Figure 4 indicates that in general this kind of approximation is not appropriate, but only simulations could give a definite answer.

4. Conclusions

We have determined the finite size contribution to the free energy $\gamma(L)$ (Eq. (10)) and the total correlation function (Eq. (6)) of a hard sphere fluid confined by two parallel hard walls at distance L. For $L \to \infty$ $\gamma(L)$ reduces to twice the wall-surface tension which compares very well with simulation data. Inspite of similarities between the structure of the inhomogeneous correlation function and its bulk counterpart significant discrepancies occur. The finite size contribution to the free energy $\gamma(L)$ shows pronounced oscillations as function of L and is consistent with values obtained via the force and the coverage relations (Eqs. (11) and (12)). The structure of the correlation function close to one wall differs significantly from that of a semi-infinite system only for narrow slits ($L \lesssim 5\sigma$).

Acknowledgements

We thank Prof. Leckerkerker for drawing our attention to the adsorption relation.

Figure captions

Figure 1: The density profile $\rho(\mathbf{R})$ (a) and the contour lines for the conditional singlet density $\rho(\mathbf{R}_1|\mathbf{R}_2) = \rho(z_2)g(r_{12}, z_1 = \sigma, z_2)$ (b) and for the radial distribution function $g(r_{12}, z_1 = \sigma, z_2)$ (d) of a hard sphere fluid close to a planar hard wall at a bulk density of $\rho_b \sigma^3 = 0.81$. For comparison also the radial distribution function $g_b(r)$ of a homogeneous hard sphere liquid at the same chemical potential is shown in (c) (note the different vertical scale). The dots and circles in (b) denote the positions of the local maxima and minima, respectively. The values of the correlation function

varies by an amount of $0.2\sigma^{-3}$ between neighbouring contour lines in (b) For reason of clarity in both cases contour lines corresponding to values larger than σ^{-3} and 1.0, respectively, are omitted.

Figure 2: The surface tension of a hard sphere fluid exposed to a single hard wall at various bulk densities ρ_b . The squares and triangles denote molecular dynamics [8] and Monte Carlo [9] simulation data, respectively. The full line represents the present results of the density functional theory within LWDA and the dotted line corresponds to the scaled particle theory [10].

Figure 3: The finite size contribution $\gamma(L)$ (Eq. (10)) to the free energy and the excess coverage $\Gamma(L)$ of a hard sphere fluid between two hard walls for various slit widths $L/\sigma = 2.025 - 6.5$ at a bulk density of $\rho_b \sigma^3 = 0.57$. In the limit $L \to \infty$ the value of $\gamma(L)$ approaches $\gamma(\infty) = -1.03/(\beta\sigma^2)$ which is twice the value shown in Fig. 2.

Figure 4: The radial correlation function $g(r_{12}, z_1 = 1.64, z_2 = z_1)$ of a hard sphere fluid in a slit of width L = 5.1 for a corresponding bulk density of $\rho_b \sigma^3 = 0.546$. It is compared with the bulk correlation function at the same density and at a reduced density $\rho(z_1 = 1.64\sigma) = 0.409/\sigma^3$, respectively. This demonstrates, that in the present case choosing the actual local density instead of the bulk density for the bulk approximation of g is even worse.

References

S. Dietrich and A. Haase, Phys. Rep. 260, 1 (1995); H. Dosch, Critical Phenomena at Surfaces and Interfaces, Springer Tracts in Modern Physics, Vol. 126 (Springer, Heidelberg, 1992).

- [2] M. D. Carbajal-Tinoco, F. Castro-Román, and J. L. Arauz-Lara, Phys. Rev. E 53, 3745 (1996).
- [3] J. L. Parker, P. Richetti, P. Kékicheff, and S. Sarman, Phys. Rev. Lett. 68, 1955 (1992).
- [4] B. K. Peterson and K. E. Gubbins, Mol. Phys. **62**, 215 (1987).
- [5] B. Götzelmann and S. Dietrich, Phys. Rev. E **55**, 2993 (1997).
- [6] B. Götzelmann, A. Haase, and S. Dietrich, Phys. Rev. E **53**, 3456 (1996).
- [7] R. Evans, J. R. Henderson, D. C. Hoyle, A. O. Parry, and Z. A. Sabeur, Mol. Phys. 80, 755 (1993).
- [8] J. R. Henderson and F. van Swol, Mol. Phys. **51**, 991 (1984).
- [9] P. Attard and G. A. Moule, Mol. Phys. **78**, 943 (1993).
- [10] H. Reiss, H. L. Frisch, E. Helfand, and J. L. Lebowitz, J. Chem. Phys. 32, 119 (1960).
- [11] J. R. Henderson, Mol. Phys. **59**, 89 (1986).
- [12] P. Tarazona, Mol. Phys. **52**, 81 (1984).
- [13] W. A. Curtin and N. W. Ashcroft, Phys. Rev. A 32, 2909 (1985).
- [14] D. Henderson and M. Plischke, Proc. R. Soc. London Ser. A 400, 163 (1985).
- [15] S. Sokołowski and J. Fischer, J. Chem. Phys. **96**, 5441 (1991).

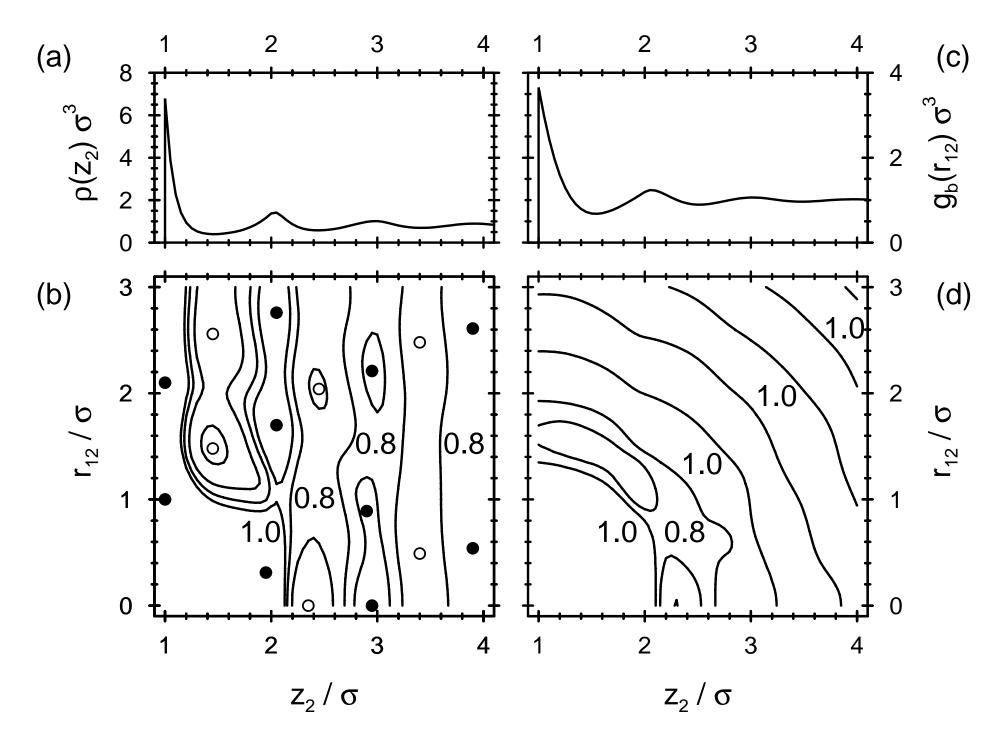


Fig. 1

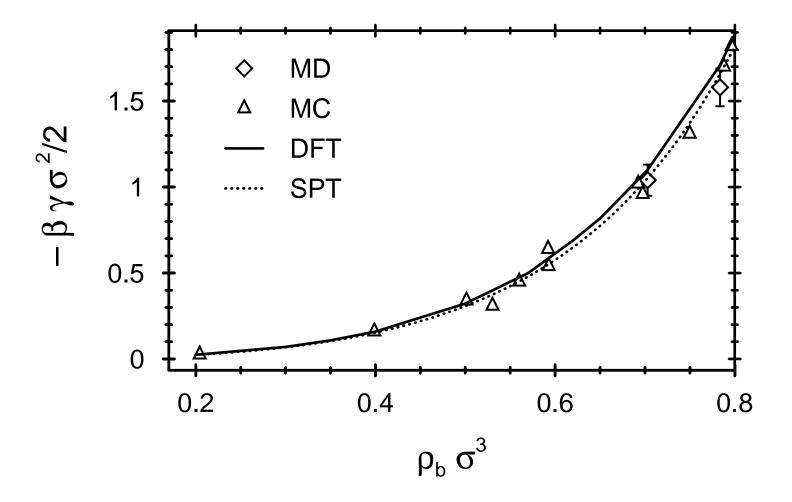


Fig. 2

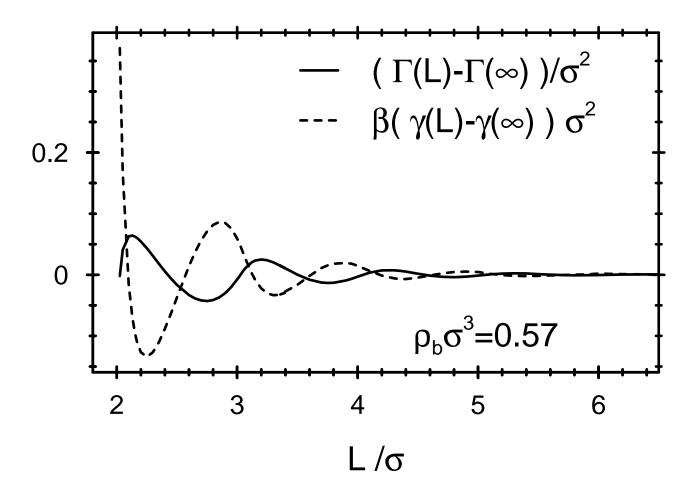


Fig. 3

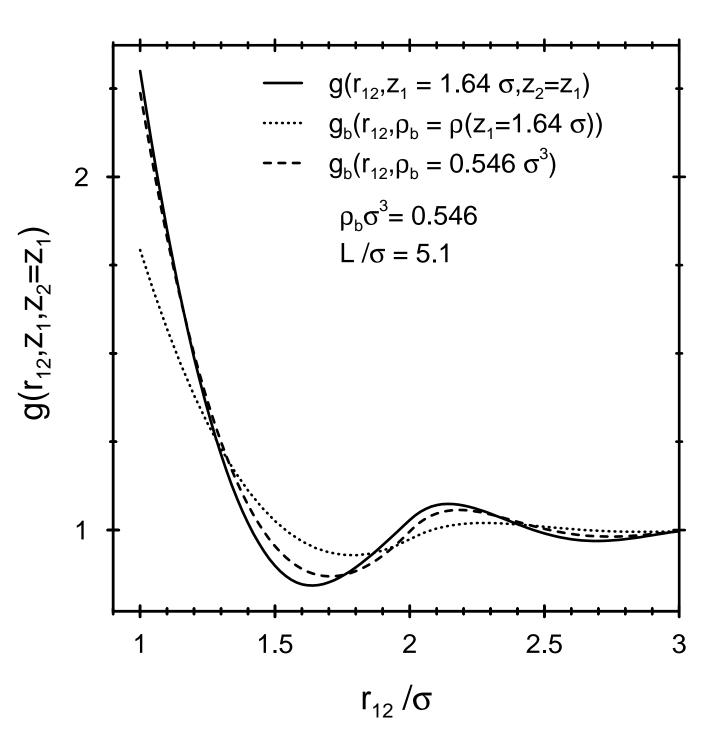


Fig. 4